

Enhancement of Photoluminescence In ZnO/GQD Nanocomposites for Bioimaging Applications

Hikmatul Gusti Fadhia Zelin, Astuti Astuti*

Material Physics Laboratory, Department of Physics, Faculty of Mathematics and Natural Sciences,
Universitas Andalas, Padang, 25163, Indonesia

Article Info

Article History:

Received January 28, 2025
Revised March 01, 2025
Accepted March 04, 2025
Published online March 05, 2025

Keywords:

ZnO
GQDs
nanocomposite
photoluminescence

Corresponding Author:

Astuti Astuti,
Email: astuti@sci.unand.ac.id

ABSTRACT

The synthesis of ZnO/GQD nanocomposites aims to increase ZnO photoluminescence by conjugating techniques with other luminescent materials, namely graphene quantum dot (GQD). This material is applied as a bioimaging material. ZnO nanoparticles were conjugated with variations of GQD, namely (0.001 g, 0.0015 g, 0.002 g) by hydrothermal method. The results of characterization of ZnO/GQD nanocomposites using XRD show the formation of a hexagonal wurzite structure of ZnO, there is no change in the crystal structure of ZnO, while GQD has an orthorhombic crystal structure. Photoluminescence shows the highest visible light emission peak of ZnO nanoparticles at a wavelength of 620 nm which produces bright yellow luminescence. ZnO/GQD nanocomposites (0.001 g, 0.0015 g, 0.002 g) produced the highest photoluminescence peaks at wavelengths of 550 nm, 590 nm, and 580 nm, respectively. From the PL results, it can be concluded that there was an increase in the photoluminescence intensity with the addition of a small amount of GQD, namely 0.001 g, and there was a shift in the photoluminescence peak towards short wavelengths. This proves that the photoluminescence characteristics of ZnO can be controlled by conjugation with GQDs. Nanocomposites ZnO/GQD potential to be developed as bioimaging material.

Copyright © 2025 Author(s)

1. INTRODUCTION

The need for biocompatible and non-toxic materials continues to increase, especially in biomedical applications. (Liu et al., 2020). One of the applications of materials in the biomedical field is as bioimaging. Bioimaging is a form of visualization or imaging of biological objects by minimizing all physical interference. Bioimaging materials are used for medical purposes such as diagnosing diseases such as cancer and heart disease. Bioimaging technology uses various strategies to analyze and solve these problems, where bioimaging techniques must be designed with the use of probes with high specificity and sensitivity. Therefore, it is necessary to explore materials that can produce images with high contrast and luminance. Materials that can be used to produce such images are luminous materials. Zinc oxide (ZnO) is one of the luminous materials that can be developed as a bioimaging material, because it is biocompatible, non-toxic, luminescence efficiency and anti-cancer properties (Rajeshkumar et al., 2019; Kumar et al., 2020). ZnO nanoparticles show very high photoluminescence in the visible light region, but the resulting photoluminescent ZnO is unstable due to defects, such as Zn or O atomic vacancies, and interstitial Zn or O, and dangling bonds on the ZnO surface (Dai et al., 2012). The luminescence of ZnO that will be utilized depend on its crystal defects and crystal structure, therefore many ways have been developed to modify ZnO crystal defects.

Conjugation of ZnO with other atoms can change the overall optical properties of ZnO nanoparticles, including their luminance (Zayed et al., 2019). ZnO conjugation with various carbon allotropes can change the optical properties of ZnO, such as ZnO conjugation with carbon quantum dot (Astuti & Usna, 2024). Besides carbon quantum dot, conjugation of ZnO nanoparticles can also be done with graphene quantum dot (GQD). GQD has good optical properties, as well as low toxicity so that it can be applied in the biomedical field. GQD can be synthesized with organic materials to reduce toxic properties that are very influential in the use of the medical field, especially bioimaging, as done by (Wang et al., 2016) who synthesized graphene from coffee grounds. Other studies synthesized GQD from rice husks using hydrothermal methods and *Opuntia* sp (Centeno et al., 2021) Combining two luminous materials such as ZnO with GQD, can produce better optical properties and is different from pure ZnO. (Wanas et al., 2023) have synthesized ZnO/GQD which can be used as a bioimaging material for tumor cells. The results obtained by GQD are effective in reducing crystal defects on the surface of ZnO. (S. Kumar et al., 2018) also conjugated ZnO with GQD using a hydrothermal method and obtained a high photoluminescence value.

Conjugation of ZnO and GQD for bioimaging applications is still limited. Therefore, it is reported here that the conjugation of ZnO with GQD can enhance the photoluminescence of ZnO so that it has the potential to be developed as a bioimaging material. The purpose of this research is to modify the optical properties of ZnO. This study also aims to determine the effect of GQD concentration on the photoluminescence properties and structure of ZnO/GQD nanocomposites. The synthesis method of ZnO and GQD used is the hydrothermal method, because it is able to produce particles with a high level of crystallinity and better control in terms of size and shape. GQD was synthesized from dried banana leaves that can be decomposed into carbon. GQD was varied in small amounts, which is expected to be effective in improving the intensity of ZnO/GQD photoluminescence.

2. METHOD

2.1 Synthesis of ZnO Nanoparticle

In this study, ZnO nanoparticles were synthesized using hydrothermal method, by mixing 0.2 M $\text{Zn}(\text{NO}_3)_2$ with 15 mL of ethanol. 2 mL of 15 mL of $\text{Zn}(\text{NO}_3)_2$ solution in ethanol was added slowly to a 15 mL solution of 0.5 M NaOH and stirred for 2 hours using a magnetic stirrer. After that, the sample was heated at 180°C for 15 hours in the oven using an autoclave (Astuti & Usna, 2024). The sample was removed in the oven and a white precipitate was obtained which was then washed three times using ethanol and distilled water, then reheated in the oven for 12 hours at 60°C.

2.2 Synthesis of Graphene Quantum Dots (GQDs)

The synthesis of GQD from dried banana leaves was carried out by hydrothermal method. Banana leaves were washed to remove dirt and dust, then dried in oven for 2 hours at 110°C to remove moisture content. After that, it is reheated using a furnace with a temperature of 400 ° C for 2 hours until it becomes charcoal (blackened) to release the existing carbon bonds. Carbon from banana leaves as much as 0.1 gram will be mixed with 10 mL of ethylene glycol and 2.5 mL of distilled water and stirred with a magnetic stirrer for 24 hours. The sample was transferred to the oven using an autoclave and heated for 6 hours at 200°C (Widiawati & Astuti, 2024). GQD solution was obtained but still contained residual hydrothermal impurities, for which centrifugation was carried out as a separation process between the sample and impurities at a speed of 300 rpm. Then the sample was filtered using 0.2 mm Wattman filter paper and the filtered solution was taken.

2.3 Synthesis of ZnO/GQDs Nanocomposite

ZnO/GQD nanocomposites were synthesized using hydrothermal method. In this method, the ZnO obtained was added to the GQD solution, and stirred using a magnetic stirrer for 2 hours. After stirring, the sample was transferred into an autoclave and heated in an oven for 4 hours at 150°C. The precipitate obtained was centrifuged and dried in an oven for 15 hours at 80°C.

2.4 Characterization

The synthesized nanocomposite was characterized using an X-ray diffractometer (Bruker D8 Advance), a UV-Vis spectrophotometer, photoluminescence (Horiba Micro Photoluminescence Microspectrometer), transmission electron microscopy (FEI Tecnai G2 20 S-Twin), and Fourier-transform infrared spectroscopy (FTIR) (Nicolet iS50). The determination of crystal size in ZnO/GQDs nanocomposite samples was calculated based on the Scherrer Equation, systematically presented in Equation (1).

$$D = \frac{K\lambda}{B\cos\theta} \quad (1)$$

where D is the nanoparticle crystalline size (nm), K is Scherrer constant (0.9), λ is wavelength of the X-ray used (nm), B is half-maximum peak width (rad) and θ is X-ray diffraction angle.

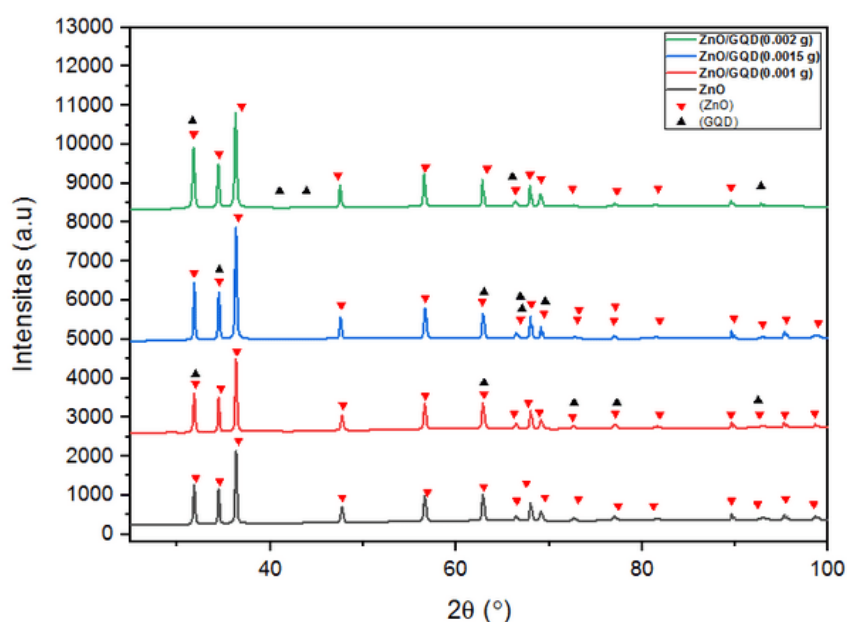


Figure 1 XRD patterns of ZnO and ZnO/GQD nanocomposites with GQD variations.

3. RESULTS AND DISCUSSION

3.1 Structure and Size Analysis

XRD characterization aims to determine the structure and size of ZnO/GQD crystals. Figure 1 presents the XRD pattern of ZnO, and ZnO/GQD nanocomposites. The results of XRD characterization of ZnO samples show diffraction peaks with the highest intensity at an angle of $2\theta = 36.29^\circ$ with results close to $2\theta = 36.29^\circ$. Based on the diffraction peaks of ZnO XRD results show similarities with the ICDD (International Center For Diffraction Data) database No. 00-005-0664. The sample formed a hexagonal wurzite crystal structure containing ZnO phase, the lattice parameters obtained are $a = b = 3.24 \text{ \AA}$ and $c = 5.20 \text{ \AA}$ and the value of $\alpha = \beta = \gamma = 90^\circ$. This indicates that the ZnO nanoparticles formed are pure ZnO without impurities.

ZnO/GQD (0.001 g) XRD pattern shows two phases, namely ZnO and C (GQD). The highest diffraction peak at an angle of $2\theta = 36.29^\circ$, identified as ZnO. Based on the data, it can be seen that there is no change in 2θ value or crystal structure of ZnO with the presence of GQD. GQD is known to have an orthorhombic structure with a lattice parameters $a = 4.5 \text{ \AA}$, $b = 5.3 \text{ \AA}$, and $c = 5.6 \text{ \AA}$ and a value of $\alpha = \beta = \gamma = 90^\circ$. The synthesis of ZnO/GQD 0.0015 g compared to the XRD results of ZnO and ZnO/GQD 0.001 g showed no significant change in the angle at the diffraction peak, namely $2\theta =$

36.27°. The compounds formed from the characterization results of ZnO/GQD 0.0015 g are ZnO and C compounds. Both ZnO and GQD do not experience changes in crystal structure in this sample, where ZnO has a hexagonal wurzite structure while GQD has an orthorhombic structure.

Table 1 Crystal size

Sample	Brad (°)	Cos 2 θ /2	D (nm)
ZnO	0,00312	0,7632	58.14
ZnO/GQD (0,001 g)	0,00312	0,7632	58.14
ZnO/GQD (0,0015 g)	0,00357	0,7468	51,22
ZnO/GQD (0,002 g)	0,00401	0,7580	46,21

XRD characterization of ZnO/GQD (0.002 g) nanocomposite show the highest diffraction peak of ZnO ($2\theta = 36.24^\circ$) There is no change in the crystal structure of ZnO or GQD, but there is a shift in the diffraction angle to be smaller than the other samples. The addition of a lot of GQD causes crystal deformation in ZnO (Sangam et al., 2018). The shift in diffraction peaks indicates a change in interplanar spacing in the crystal lattice. This is caused by several factors such as strain, temperature, and changes in crystal size. In this case, the shift in diffraction peaks is caused by changes in crystal size due to the addition of GQD. Where the diffraction peak shifts to a lower angle, which is caused by lattice expansion. The XRD data shows a decrease in the diffraction angle from $2\theta = 36.29^\circ$ to $2\theta = 36.24^\circ$, which goes hand in hand with an increase in the interplanar spacing from 2.47 Å to 2.49 Å. The addition of GQD also causes a decrease in ZnO diffraction intensity because GQD covers the surface of the ZnO crystal (EL-Dafrawy et al., 2021).

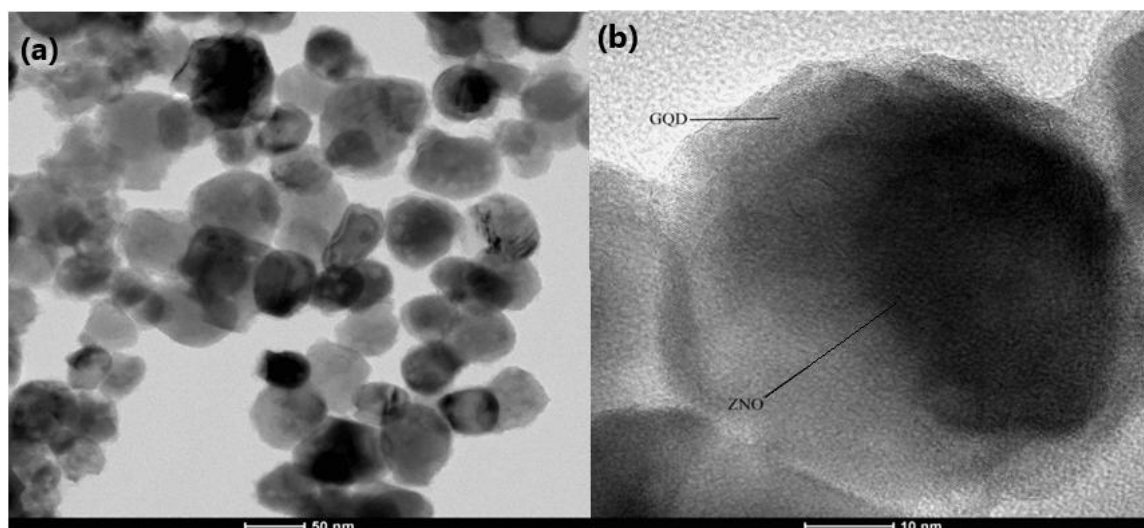


Figure 2. TEM images of the ZnO/GDQ (0,002 g) (a) Low ratio, (b) High ratio

The crystal size of ZnO nanoparticles and ZnO/GQD nanocomposite was determined using the Scherrer equation (Equation 1). The crystal size calculation of ZnO nanoparticles and ZnO/GQD nanocomposites are shown in Table 1. The crystal size of ZnO was found to be 58.14 nm. The ZnO/GQD nanocomposite of 0.0015 g obtained a crystal size of 51.22 nm. The results of the crystal size of ZnO/GQD 0.0015 g show that the addition of GQD can reduce the crystal size, this is due to the formation of heterostructures from GQD (Mandal et al., 2021).

The particle size was characterized using HR-TEM. The TEM test results are shown in Figure 2. Figure 2 shows ZnO/GQD nanocomposite particles with spherical morphology which are ZnO nanoparticles. Furthermore, ZnO is coated by a hexagon-patterned sheet of GQD. The average particle size of ZnO/GQD nanocomposite is 70 nm.

2.2 FTIR analysis

FTIR characterization was performed on ZnO/GQD nanocomposite material with variations of GQD 0.001 g, 0.0015 g, 0.002 g. This characterization aims to see the functional groups contained in the ZnO/GQD nanocomposite. The FTIR spectrum uses wave numbers 400 cm^{-1} to 4500 cm^{-1} . The test results show transmission peaks related to the vibrational energy seen in Figure 3.

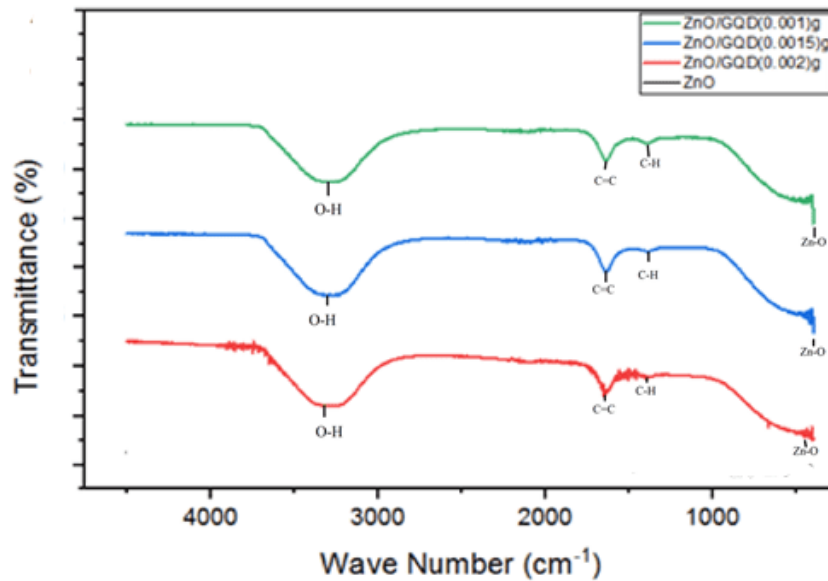


Figure 3. FTIR spectra of ZnO/GQD

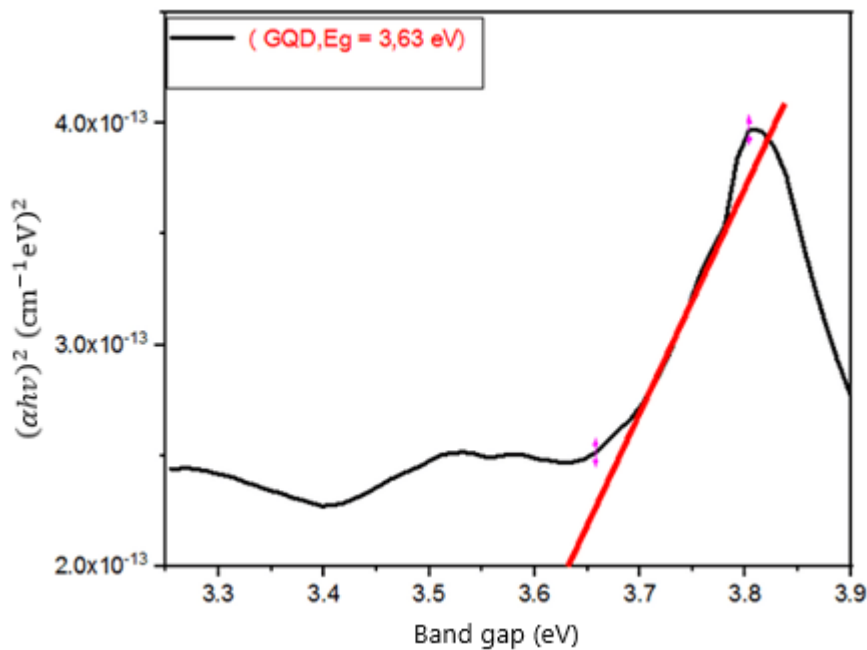


Figure 4 Absorbance spectra of $\text{Fe}_3\text{O}_4/\text{ZnO}$ nanocomposite and $\text{Fe}_3\text{O}_4/\text{ZnO} / \text{GQDs}$ nanocomposite with isopropanol variation

All ZnO/GQD nanocomposite samples with GQD variations of 0.001 g, 0.0015 g and 0.002 g have an O-H functional group around 3263.56 cm^{-1} which indicates the absorption of water molecules in ZnO nanoparticles. The C=C group bond is at a wavelength of about 1649.14 cm^{-1} . This peaks indicate the formation of GQD, as C=C is the main functional group in GQD (da Costa et al., 2018; Wanas et al., 2023). The absorption region at a wavelength of about 1388.75 cm^{-1} indicates the presence of C-H functional groups and Zn-O bond at wavelengths ($422.42, 451.34, 480.28, 507.28, 599.86$) cm^{-1} . The presence of Zn-O and C=C functional groups indicates that ZnO and GQD are formed in ZnO/GQD nanocomposites by the hydrothermal method (Liang et al., 2020).

3.3 UV-Vis Spectrophotometer Analysis

Further characterization uses a UV-Vis spectrophotometer to determine the width of the energy band gap in the GQD sample. UV-Vis characterization results display the value of wavelength (nm) against absorbance (a.u). The measurement of the absorbance spectrum of GQD is shown in Figure 4. The red straight line shows the extrapolation of the graph to the X-axis. The intersection point of this line with the X-axis gives the energy band gap (E_g) value of GQD, which is 3.63 eV. The GQD energy gap result reported here is slightly lower than the GQD energy gap value obtained by (Martínez-Rovira et al., 2019) which is close to 3.68 eV.

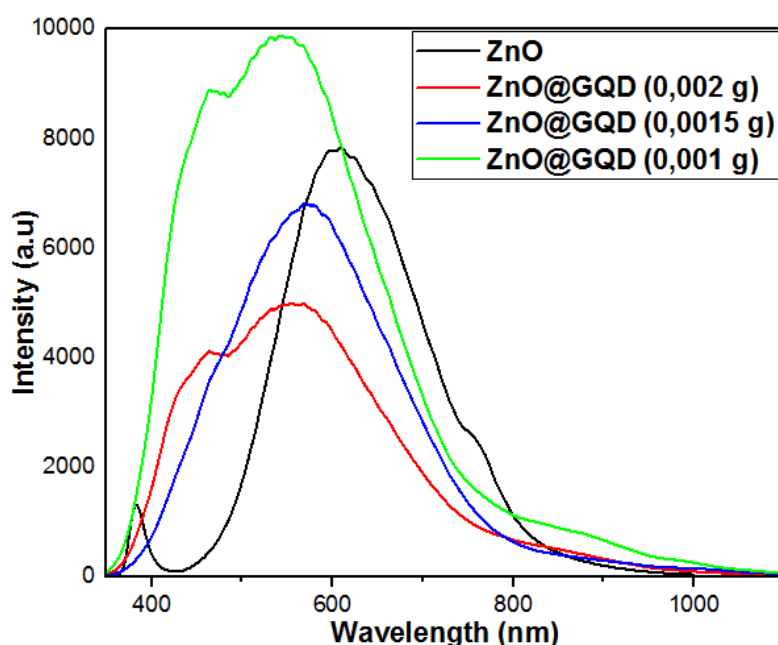


Figure 5 Photoluminescence result of ZnO nanoparticle and ZnO/GQDs nanocomposite

3.4 Photoluminescence (PL) Spectroscopy Analysis

PL characterization was performed to determine the luminescence properties of ZnO and ZnO/GQD nanocomposites. The results obtained from this test are the emission intensity of ZnO, ZnO/GQD (0.001 g, 0.0015 g, 0.002 g) against the wavelength value. PL characterization results were obtained by firing 325 nm laser light to produce the spectrum.

Figure 5 displays the photoluminescence spectra produced by ZnO and ZnO/gQD nanocomposite variants having wavelengths from 300 nm to 1000 nm and showing different intensities as in the appendix. The emission peaks are broad in the range of 500-700 nm. ZnO light emission peaks at a wavelength of 620 nm that show yellow emission. The yellow emission was caused by the electron transition from ZnI to the oxygen vacancy state (V_O).

In the photoluminescence (PL) results of ZnO material there is a small peak at a wavelength of 400 nm that is Near Band Edge (NBE) and Deep Level Emission (DLE) are the two main emission mechanisms each associated with a specific electron transition in the ZnO energy structure. NBE

originates from the recombination of excitons (electron-hole pairs) near the band edge of ZnO. It is usually in the ultraviolet (UV) region with a wavelength of about 370-380 nm. This emission indicates the crystalline quality of ZnO and the presence of slight structural defects. A strong NBE intensity indicates that the material has a high degree of crystallinity (Özgür et al., 2005). DLE emission comes from electron transitions between defect levels in the band gap and is usually in the visible region (green, yellow, or red) with longer wavelengths (lower energy) than NBE. This emission occurs due to defects such as oxygen vacancy (V_O), zinc vacancy (V_{Zn}), interstitial zinc (Zni), or interstitial oxygen (Oi) (Vanheusden et al., 1997).

When GQDs are added to ZnO materials, the phenomenon of disappearance or weakening of DLE and NBE emissions in the photoluminescence results can be caused by several physical and chemical mechanisms. GQDs have electron donor or acceptor properties. When GQD is combined with ZnO, electron transfer occurs between GQD and ZnO due to the difference in energy levels. So that electrons that previously contributed to the recombination of NBE excitons or recombination in DLE defects will be transferred to GQD. As a result, the intensity of PL emission from NBE and DLE decreases or even disappears because the formation of electron-hole pairs is disrupted (Shen et al., 2013). GQDs can cover the ZnO surface or bind to defects such as oxygen vacancy (V_O) and zinc vacancy (V_{Zn}), the impact of which is non-radiative recombination associated with defects where the main cause of DLE is reduced. DLE disappears because the defects responsible for the emission have been passivated. GQD can modify the energy band structure of ZnO through doping interactions, the energy level of defects in ZnO changes due to doping, so that the electron transition that produces DLE does not occur (Astuti & Usna, 2024). The emission peaks from the variation of GQD solution volume on the ZnO/GQD nanocomposite show an increase in visible emission at 550 nm, 590 nm, and 580 nm. The emission peak widens in the visible light range from 500 nm to 800 nm, this is due to the addition of GQD. The addition of GQD causes a shift of the emission peak to short wavelengths, i.e. 550-590 nm, in the green emission range. This happens because GQD itself is green emission when illuminated by UV light and GQD can change the band gap of ZnO through electron transfer or the formation of new bonds. This can increase the effective band gap energy, which results in light emission at shorter wavelengths (Centeno et al., 2021). The highest emission peak in the ZnO/GQD nanocomposite variation is at a wavelength of 550 nm, which produces a green emission. The presence of carbon atoms in the 0.001 g ZnO/GQD nanocomposite sample has the highest intensity, because the addition of GQD can increase the surface area of ZnO and change the optical properties of ZnO.

4. CONCLUSION

ZnO/GQD nanocomposites have been successfully synthesized using hydrothermal method. XRD, TEM, FTIR, UV-Vis and Photoluminescence (PL) characterization results confirmed the effect of GQD concentration on the structure and photoluminescent properties of ZnO/GQD. The addition of a small amount of GQD (0.001 g) to ZnO can increase its photoluminescence intensity. In addition, there is also a shift in the emission band towards short wavelengths due to the addition of GQD. ZnO without GQD has an emission peak of 620 nm which produces yellow color photoluminescence. After the addition of GQD, the emission peak shifts to wavelengths in the range of 550 nm-590 nm which produces green photoluminescence. This proves that the photoluminescence of ZnO/GQD nanocomposites can be regulated by the addition of a certain amount of GQD. Based on the results obtained, the ZnO/GQD nanocomposite has the potential to be developed as a bioimaging material.

ACKNOWLEDGEMENT

This research was supported by the provision of research equipment in the materials physics laboratory at Andalas University.

REFERENCE

- Astuti, A., & Usna, S. R. A. The Influence of Carbon Quantum Dots Addition on the Photoluminescence Performance of ZnO Nanoparticles. *Scientia Iranica*, <https://doi.org/10.24200/sci.2024.63810.8610>. in press
- Centeno, L., Romero-García, J., Alvarado-Canché, C., Gallardo-Vega, C., Télles-Padilla, G., Díaz Barriga-Castro, E., Cabrera-Álvarez, E. N., Ledezma-Pérez, A., & de León, A. (2021). Green synthesis of graphene quantum dots from *Opuntia* sp. extract and their application in phytic acid detection. *Sensing and Bio-Sensing Research*, *32*, 100412. <https://doi.org/10.1016/j.sbsr.2021.100412>
- da Costa, R. S., da Cunha, W. F., Pereira, N. S., & Ceschin, A. M. (2018). An alternative route to obtain carbon quantum dots from photoluminescent materials in peat. *Materials*, *11*(9), 12–17. <https://doi.org/10.3390/ma11091492>
- Dai, K., Dawson, G., Yang, S., Chen, Z., & Lu, L. (2012). Large scale preparing carbon nanotube/zinc oxide hybrid and its application for highly reusable photocatalyst. *Chemical Engineering Journal*, *191*, 571–578. <https://doi.org/10.1016/j.cej.2012.03.008>
- EL-Dafrawy, S. M., Tarek, M., Samra, S., & Hassan, S. M. (2021). Synthesis, photocatalytic and antidiabetic properties of ZnO/PVA nanoparticles. *Scientific Reports*, *11*(1), 1–11. <https://doi.org/10.1038/s41598-021-90846-8>
- Kumar, S., Dhiman, A., Sudhagar, P., & Krishnan, V. (2018). ZnO-graphene quantum dots heterojunctions for natural sunlight-driven photocatalytic environmental remediation. *Applied Surface Science*, *447*, 802–815. <https://doi.org/10.1016/j.apsusc.2018.04.045>
- Kumar, Y. R., Deshmukh, K., Sadasivuni, K. K., & Pasha, S. K. K. (2020). Graphene quantum dot based materials for sensing, bio-imaging and energy storage applications: a review. *RSC Advances*, *10*(40), 23861–23898. <https://doi.org/10.1039/d0ra03938a>
- Liang, H., Tai, X., Du, Z., & Yin, Y. (2020). Enhanced photocatalytic activity of ZnO sensitized by carbon quantum dots and application in phenol wastewater. *Optical Materials*, *100*(October 2019), 109674. <https://doi.org/10.1016/j.optmat.2020.109674>
- Liu, J., Kotrchová, L., Lécuyer, T., Corvis, Y., Seguin, J., Mignet, N., Etrych, T., Scherman, D., Randárová, E., & Richard, C. (2020). Coating Persistent Luminescence Nanoparticles With Hydrophilic Polymers for in vivo Imaging. *Frontiers in Chemistry*, *8*(September), 1–10. <https://doi.org/10.3389/fchem.2020.584114>
- Mandal, S. K., Paul, S., Datta, S., & Jana, D. (2021). Nitrogenated CQD decorated ZnO nanorods towards rapid photodegradation of rhodamine B: A combined experimental and theoretical approach. *Applied Surface Science*, *563*(June), 150315. <https://doi.org/10.1016/j.apsusc.2021.150315>
- Martínez-Rovira, I., Seksek, O., & Yousef, I. (2019). A synchrotron-based infrared microspectroscopy study on the cellular response induced by gold nanoparticles combined with X-ray irradiations on F98 and U87-MG glioma cell lines. *Analyst*, *144*(21), 6352–6364. <https://doi.org/10.1039/c9an01109a>
- Özgür, Ü., Alivov, Y. I., Liu, C., Teke, A., Reshchikov, M. A., Doğan, S., Avrutin, V., Cho, S. J., & Morkoç, H. (2005). A comprehensive review of ZnO materials and devices. *Journal of Applied Physics*, *98*(4), 1–103. <https://doi.org/10.1063/1.1992666>
- Rajeshkumar, S., Menon, S., Venkat Kumar, S., Tambuwala, M. M., Bakshi, H. A., Mehta, M., Satija, S., Gupta, G., Chellappan, D. K., Thangavelu, L., & Dua, K. (2019). Antibacterial and antioxidant potential of biosynthesized copper nanoparticles mediated through *Cissus arnotiana* plant extract. *Journal of Photochemistry and Photobiology B: Biology*, *197*(April). <https://doi.org/10.1016/j.jphotobiol.2019.111531>
- Sangam, S., Gupta, A., Shakeel, A., Bhattacharya, R., Sharma, A. K., Suhag, D., Chakrabarti, S., Garg, S. K., Chattopadhyay, S., Basu, B., Kumar, V., Rajput, S. K., Dutta, M. K., & Mukherjee, M. (2018). Sustainable synthesis of single crystalline sulphur-doped graphene quantum dots for bioimaging and beyond. *Green Chemistry*, *20*(18), 4245–4259. <https://doi.org/10.1039/c8gc01638k>
- Shen, C., James, S. A., De jonge, M. D., Turney, T. W., Wright, P. F. A., & Feltis, B. N. (2013). Relating cytotoxicity, zinc ions, and reactive oxygen in ZnO nanoparticle-exposed human immune cells. *Toxicological Sciences*, *136*(1), 120–130. <https://doi.org/10.1093/toxsci/kft187>
- Vanheusden, K., Seager, C. H., Warren, W. L., Tallant, D. R., Caruso, J., Hampden-Smith, M. J., & Kodas, T. T. (1997). Green photoluminescence efficiency and free-carrier density in ZnO phosphor powders prepared by spray pyrolysis. *Journal of Luminescence*, *75*(1), 11–16. [https://doi.org/10.1016/S0022-2313\(96\)00096-8](https://doi.org/10.1016/S0022-2313(96)00096-8)
- Wanas, W., Abd El-Kaream, S. A., Ebrahim, S., Soliman, M., & Karim, M. (2023). Cancer bioimaging using dual mode luminescence of graphene/FA-ZnO nanocomposite based on novel green technique. *Scientific Reports*, *13*(1). <https://doi.org/10.1038/s41598-022-27111-z>

- Wang, L., Li, W., Wu, B., Li, Z., Wang, S., Liu, Y., Pan, D., & Wu, M. (2016). Facile synthesis of fluorescent graphene quantum dots from coffee grounds for bioimaging and sensing. *Chemical Engineering Journal*, 300, 75–82. <https://doi.org/10.1016/j.cej.2016.04.123>
- Widiawati, S., & Astuti, A. (2024). Effect of Isopropanol on Optical Properties of Fe₃O₄ / ZnO / Graphene Quantum Dots (GQDs) Nanocomposite. *Jurnal Ilmu Fisika*. 16(2), 142–150.
- Zayed, D. G., Ebrahim, S. M., Helmy, M. W., Khattab, S. N., Bahey-El-Din, M., Fang, J. Y., Elkhodairy, K. A., & Elzoghby, A. O. (2019). Combining hydrophilic chemotherapy and hydrophobic phytotherapy via tumor-targeted albumin-QDs nano-hybrids: Covalent coupling and phospholipid complexation approaches. *Journal of Nanobiotechnology*, 17(1), 1–19. <https://doi.org/10.1186/s12951-019-0445-7>